Nonlocal competition and logistic growth: Patterns, defects, and fronts

Yosef E. Maruvka and Nadav M. Shnerb

Department of Physics, Bar-Ilan University, Ramat-Gan 52900 Israel
(Received 12 June 2005; published 10 January 2006)

Logistic growth of diffusing reactants on spatial domains with long-range competition is studied. The bifurcations cascade involved in the transition from the homogeneous state to a spatially modulated stable solution is presented, and a distinction is made between a modulated phase, dominated by single or few wave numbers, and the spiky phase, where localized colonies are separated by depleted region. The characteristic defects in the periodic structure are presented for each phase, together with the invasion dynamics in the case of local initiation. It is shown that the basic length scale that controls the bifurcation is the width of the Fisher front, and that the total population grows as this width decreases. A mix of analytic results and extensive numerical simulations yields a comprehensive examination of the possible phases for logistic growth in the presence of nonlocal competition.

I. INTRODUCTION

Recently, there is a growing interest in the spatial properties of logistic growth with nonlocal interactions. Interestingly, some results have been published independently by authors from different disciplines, ranging from pure mathematics to ecological modeling [1–15]. A variety of models have been introduced, including various types of interaction kernels, deterministic and stochastic evolution, and growth or death rate that depends on the local population. A common feature found in all these models is the *segregation transition*, i.e., for small enough diffusion and for certain interaction kernels the homogeneous state of the system becomes unstable and the steady state is spatially heterogeneous. This feature turns out to be stable against the stochasticity induced by the discrete nature of the reactants, and the total carrying capacity (per unit volume) of the stochastic system depends on the details of the spatial segregation [7,15].

In previous work [6], the general conditions for the integral kernel to allow for spatial segregation have been presented, and the existence of topological defects between ordered domains has been analyzed in detail for a logistic growth on a one dimensional array of patches with nearest neighbor competition. Here, a comprehensive study of this reaction-diffusion equation is presented: short-range interactions are shown to yield spatial modulation of arbitrary large wavelength and different types of defects, the total population of the system admits nontrivial dependence upon the diffusion rate, and the dynamics of the system is studied, both for global initiation and for local initiation. The appearance of domains with different order parameters and the features of the boundaries between them is considered in detail for various situations.

Our starting point is the well-investigated Fisher–Kolomogoroff-Petrovsky-Piscounoff (FKPP) equation [16,17], first introduced by Fisher to describe the spreading of a favored gene in population:

$$\frac{\partial c(x,t)}{\partial t} = D\nabla^2 c(x,t) + ac(x,t) - bc^2(x,t). \quad (1)$$

Clearly, this equation is a straightforward generalization of the logistic growth to spatial domains, and allows for two steady states: an unstable state with $c(x)=0 \ \forall \ x$ and the stable steady state $c(x)=a/b$. It was shown that, for any local initiation of the system [i.e., $c(x) \neq 0$ on a compact domain], the invasion of the stable phase into the unstable region takes place via a front that moves in a constant velocity $v_F = 2\sqrt{Da}$. The stability of this solution, the fact that the velocity is determined by the leading edge ("pulled front") and the corrections to this expression due to stochastic noise associated with the discrete nature of the reactants [18], has been reviewed, recently, by various authors [19].

The FKPP equation is the simplest equation that describes the transition from unstable to stable steady state on spatial domains, and as such it fits many situations, from the spread of a disease by infection to the advance of a fire or new technology. Accordingly, this model has been widely studied from many points of view and has been generalized in many directions such as modified interaction terms, nonlinear diffusion, and so on.

The process considered here, logistic growth with nonlocal competition, is described by the generalized FKPP equation:

$$\frac{\partial c(x,t)}{\partial t} = D\nabla^2 c(x,t) + ac(x,t) - c(x,t)\int_{-\infty}^{\infty} \gamma(x,y)c(y,t)dy, \quad (2)$$

where $\gamma(x,y)$ is the interaction kernel, and the original FKPP process corresponds to the limit $\gamma(x,y)=\delta(x-y)$.

The motivation for the study of this process comes from one of the basic mechanisms in population growth, namely, the competition for common resource. In any autocatalytic system the multiplication of agents depends on various resources (energy, chemicals, water, etc.). If there is only a limited amount of the resource, its consumption leads to extinction, so generally any crucial resource should be deposited, and its availability dictates the saturation value for the population. As a concrete example let us look at vegetation [20–22]: the common resource needed for vegetation is water, and the rain corresponds to deposition of this resource. If
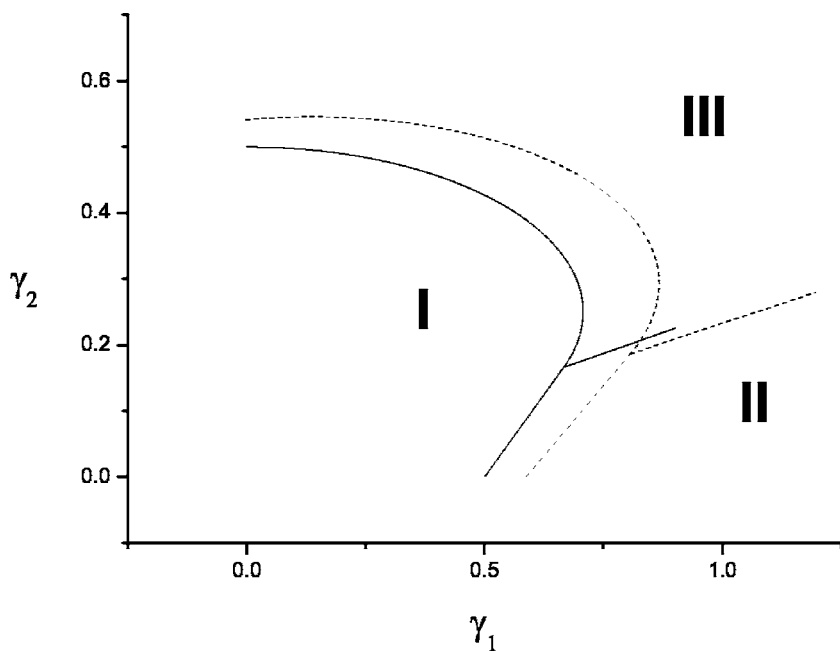
FIG. 1. Phase diagram for next nearest neighbor competition at $D=0$ (solid line) and $D=0.02$ (dashed line). Region I is the homogeneous, while II marks the up-down stable solution region similar to the nearest neighbor case. In region III the wave vector k_3 (defined in the text) is stable and various wave numbers may be active. As diffusion increases the homogeneous region "blows up" since the instability appears only for stronger competition, as implied by Eq. (15).

the resource dynamics is much faster than that of the agents (shrubs, trees, etc.), there is, at any time, a soil moisture profile that reflects the instantaneous vegetation configuration, and there is a depletion of this moisture at the spatial region around a biomass unit. Accordingly, the environmental conditions for a new agent at this region becomes hostile. Following arguments of this type one suggests that *competition for common resource induces long-range competition among agents via the depletion of the resource in the surroundings of an agent*. Other examples may involve the competition for light [23], foraging of the predator that induces an effective coupling between prey habitats [24], and cooperation among agents (symbiosis) that may yield "negative competition" among the reactants.

Two length scales play a role in our modeling: the first is a short length associated with the discreteness of the reactants and the second is the competition length. As any natural phenomenon involves discrete objects, there is a basic length associated, for example, with the size of the creature, the diameter of a single perennial shrub, or the typical distance between habitats. The competition is "long range" only if the competition length is larger than this short length cutoff. Accordingly, the model presented here is a lattice model, where a single patch is associated with the basic natural unit and the lattice constant is the corresponding short scale (see, e.g., Ref. [24]). The competition range is then measured in these units. As explained in the next section, another length scale, the width of the Fisher front, appears due to the *dynamics* of the invasion and dictates the transition to the continuum limit.

The numerical procedure for simulations of the dynamics corresponding to Eq. (2) require space and time discretization. In this work the time evolution of the system is generated via forward Euler integration, where the time step is taken small enough such that further reduction of it does not affect the results. The system is simulated on discrete patches with periodic boundary conditions, where the hopping rate is proportional to the diffusion constant.

Let us present some *a priori* considerations related to this system. There are few basic types of steady state solutions: first, it may happen that the steady state is *homogeneous*: this may be the case if the long-range competition is too weak, or if the interaction kernel does not allow for the instability to occur [4,6]. At some point in the parameter region the homogeneous solution becomes unstable against perturbation with one specific wavelength, the spatial symmetry breaks and modulation at this wavelength appears. At this point, i.e., along the line in parameter space that defines the stability limit of the homogeneous state, only a single wavelength admits negative Lyapunov exponent and dictates the inhomogeneous (modulated) steady state. Far from this line (see the phase diagram plotted in Fig. 1 below) the homogeneous state is unstable against many wavelengths, perturbations of different modulations grow in time, and some sort of mode competition takes place. Still, if the parameters are close to the stability limit there will be one wavelength that dominates the system and suppresses all other "active" modes. Far from this line there is strong competition and the steady state is no longer dominated by a single wavelength. Instead, if the competition is strong enough in some range one may expect that "life" at a single patch forces all the other patches at this finite range to be (almost) empty, and the steady state corresponds to a lattice of almost isolated colonies ("spikes") where many active wavelengths participate in the formation of localized bumps.

As we are looking at a dynamical system with no noise, few stable steady states may exist simultaneously, each admits its own basin of attraction in the space of possible initial conditions. Numerically, however, it turns out that only one important distinction should be made, namely, between local and global initiation: the initiation is "local" if at $t=0$ there is finite support to the colony, while if the system begins with random small biomass that spreads all around it corresponds to global initiation. Within each of these subclasses, the numerics suggests that a generic initial condition flows into a specific steady state.

This paper is organized as follows: in the second section the stable spatial configurations (steady states stable against small fluctuations) are presented: the conditions for an instability of the homogeneous solution are reviewed and discussed, and the properties of the final state are identified in different parameter regions, leading to a characteristic "phase diagram." In the next section the appearance of defects (separating spatial regions with different order parameter phase) is studied. The fourth section deals with the "spiky" phase, where many excited modes superimposed to yield a pattern of spikes and the typical defect is a combination of two depletion regions. In the fifth section there is a brief description of phases and defects in two spatial dimensions, and in the next section the effect of the spatial segregation on the global population is considered. In the seventh section the dynamic properties of the model are discussed, including the velocity of the primary and the secondary Fisher fronts and the appearance of topological defect in the invaded region. Some comments and conclusions are presented at the end.

II. STATIC PROPERTIES

In this section we consider the steady state solutions for Eq. (2) on spatial domain of coupled, identical patches. The initiation is assumed to be *global*, i.e., the initial conditions are small, randomly spread, a reactant population at each spatial patch. The model considered here allows for nontrivial spatial organization even in the absence of diffusion, due to the long-range competition, and global initiation helps us to see these features within reasonable simulation times. The differences, if any, between global and local initiation will be considered in the last section.

A. Bifurcation cascade

Let us consider the spatially discretized version of Eq. (2), i.e., an infinite one dimensional array of identical patches coupled to each other by diffusion and long-range competition. The time evolution of the reactant density at the nth site, $\tilde{c}_n$, is given by

$$\frac{\partial \tilde{c}_n(t)}{\partial t} = \frac{\tilde{D}}{l_0^2}[-2\tilde{c}_n(t) + \tilde{c}_{n+1}(t) + \tilde{c}_{n-1}(t)] + a\tilde{c}_n(t) - b\tilde{c}_n^2(t)$$

$$- \tilde{c}_n(t)\sum_{r=1}^{\infty} \tilde{\gamma}_r[\tilde{c}_{n+r}(t) + \tilde{c}_{n-r}(t)], \qquad (3)$$

where $\tilde{D}$ is the diffusion constant and a, b, $\tilde{\gamma}$ are the corresponding reaction coefficients (for the sake of clarity an explicit distinction is made between the "usual" on-site logistic saturation coefficient b and the nonlocal competition $\tilde{\gamma}$). One may define the dimensionless quantities

$$\tau = at, \quad c = b\tilde{c}/a, \quad \gamma_r = \tilde{\gamma}_r/b, \quad D = \frac{\tilde{D}}{al_0^2}. \qquad (4)$$

Note that the new "diffusion constant" is $D=W^2/l_0^2$, where $W \equiv \sqrt{D/a}$ is the width of the Fisher front, so the dimension-

less diffusion is determined by the ratio between the front width and the lattice constant. The continuum limit, though, is the limit where the front width is large in units of lattice spacing. With these definitions Eq. (3) takes its dimensionless form,

$$\frac{\partial c_n}{\partial \tau} = D[-2c_n + c_{n+1} + c_{n-1}]$$

$$+ c_n\left(1 - c_n - \sum_{r=1}^{\infty} \gamma_r[c_{n+r} + c_{n-r}]\right), \qquad (5)$$

that may be expressed in Fourier space [with $A_k \equiv \Sigma_n c_n e^{iknl_0}$] as

$$\dot{A}_k = \alpha_k A_k - \sum_q \beta_{k-q} A_q A_{k-q}, \qquad (6)$$

where

$$\alpha_k \equiv 1 - 2D[1 - \cos(kl_0)], \qquad (7)$$

$$\beta_k \equiv 1 + 2\sum_{r=1}^{\infty} \gamma_r \cos(rkl_0). \qquad (8)$$

Following Ref. [26], one observes that c_n is positive semidefinite so A_0 is always "macroscopic." Any mode is suppressed by A_0; accordingly, for small γ_r one expects only the zero mode to survive. If, on the other hand, γ_r increases above some threshold, bifurcation may occur with the activization of some other k mode(s), and the homogenous solution becomes unstable.

Instability occurs if a k mode exists such that small perturbation with wavelength $2\pi/k$ grows in time. Linear stability analysis of a single k mode in the presence of A_0 leads to the equation

$$\dot{A}_k = 1 - 2D[1 - \cos(kl_0)]A_k - \beta_k A_0 A_k - \beta_0 A_k A_0. \qquad (9)$$

A_k is positive, so bifurcation occurs when

$$1 - 2D[1 - \cos(kl_0)] - \beta_k A_0 - \beta_0 A_0 > 0, \qquad (10)$$

where the homogeneous solution is $A_0 = 1/\beta_0$. A modulation k grows if

$$g(k) \equiv \beta_k + 2\beta_0 D[1 - \cos(kl_0)] < 0 \qquad (11)$$

is fulfilled for that k. This is the situation where patterns appear and translational symmetry breaks. Right above the bifurcation there is only one "active" k mode that dictates the modulation of the system. As $g(k)$ decreases further there are many active modes that compete with each other via the nonlinear terms of Eq. (6), and the linear stability analysis of the homogeneous state may be irrelevant to the final spatial configuration.

B. Nearest neighbor interactions

In previous work [6], the properties of the system have been considered for the extreme case where the competition takes place only between neighboring sites ($\gamma_r = \gamma$ for $r=1$

and $\gamma_r=0$ if $r>1$). For nearest neighbor (NN) interaction of that type the only stable wave number is $k=\pi/l_0$, where l_0 is the lattice constant, and the bifurcation takes place at $\gamma=1/2$. The spatial state at this wave number is $u_n=A_0+A_\pi\cos(n\pi/l_0)$ and the spatial structure is of the form $\cdots ududud\cdots$ (u=up, large amount of biomass, d=down, small amount). In the absence of diffusion spatial segregation takes the form 101010, i.e., only the even (odd) sites are populated. Obviously, starting from generic random state different domains are created with odd or even "order parameter" and kinks (domain walls) emerge between different domains. As shown in Ref. [6], the structure of these topological defects, including their size (that diverges at the segregation transition) and their exact form, may be calculated analytically.

C. Next nearest neighbors (NNN)

Quite surprisingly, the increase of the competition radius by a single site takes us to a completely different regime. While in the case of nearest neighbor interaction the spatial modulation length and the competition length are the same, next nearest neighbor competition (and, accordingly, any interaction of longer range) may yield, upon tuning the parameters, spatial modulation of arbitrary large wavelength. This situation resembles the case of magnetic systems, e.g., an Ising chain: if the exchange interaction is only between nearest neighbors the equilibrium state admits only an up-down modulation, while NNN interaction may yield large solitons, as shown by Ref. [25]. In that sense the next NN case demonstrates the essential features of the long-range competition

model in a generic way, while at least part of the results may be inferred analytically.

The most general form of next nearest neighbor interactions is given by Eq. (5) with

$$\gamma_r = \begin{cases} \gamma_1, & r=1 \\ \gamma_2, & r=2 \\ 0, & \text{else}. \end{cases} \tag{12}$$

The bifurcation threshold is defined now by the equation [using Eq. (11) and the explicit expression for β_k]:

$$g(k) = 1 + 2\gamma_1\cos(kl_0) + 2\gamma_2\cos(2kl_0) + 2\beta_0 D[1-\cos(kl_0)]$$

$$= 0, \tag{13}$$

where g has extremum points at $k_{1,2}=0,\pi$ and

$$k_3 = \arccos\left(\frac{-\gamma_1+\beta_0 D}{4\gamma_2}\right). \tag{14}$$

If a real wave vector k_3 exists [i.e., at $|(-\gamma_1+\beta_0 D)/4\gamma_2|<1$] it is the minimum of $g(k)$ while $k_{1,2}$ are maxima. For the range of parameters where k_3 is imaginary the minima may be at $k=\pi$ and the modulation is of "up-down" type, or at $k=0$, where the homogeneous state is stable. The resulting phase diagram, in the γ_1-γ_2 plane with zero diffusion, is presented by the solid line in Fig. 1: In region I the homogeneous state is stable, while in region II the bifurcation takes the system to the up-down mode, like the situation for NN interaction. In region III, however, k_3 dominates and modulations of any size may occur. The bifurcation line is given (in the presence of diffusion) by the two branches of the equation:

$$\gamma_2 = \frac{1+2D-D^2+\gamma_1(5D-2D^2)\pm\sqrt{1+4D+14D\gamma_1-2\gamma_1^2+12D\gamma_1^2}}{2D^2+4-16D} \tag{15}$$

that reduces, at the $D=0$ case, to the simple form

$$\gamma_2 = \frac{1\pm\sqrt{1-2\gamma_1^2}}{4}. \tag{16}$$

1. Wavelength selection, mode competition, and the spiky phase

From Eq. (13) it seems that the bifurcation wavelength is bounded from above by the interaction length (no minima at nontrivial k exists above the interaction length, as all terms of the derivative are of the same sign). This, however, is not the actual situation on a discrete lattice: the wavelength inferred from Eq. (14), although bounded, is generically incommensurate with the lattice constant, and the system should choose a commensurate one. It turns out that, if the wavelength is rational (i.e., if $k_3=2\pi m/n$, where m and n admits no common denominator) the spatial modulation re-

peats itself after n lattice sites. A typical example is the steady state obtained numerically for the case $m=7$, $n=20$ where a period-20 modulation appears, as demonstrated in Fig. 2. At finite system the maximal n allowed is of order of the system size, and only in an infinite system all rational fractions may be activated. Note that in an infinite system any change of the interaction parameters yields different wavelengths, a phenomenon that resembles the "devil staircase" situation in spin systems [25].

For a finite system thus there is a set of points along the bifurcation line that corresponds to the allowed wavelengths. Numerical simulation indicates that there is a basin of attraction around each of these points, i.e., if the interaction parameters γ_1 and γ_2 yield a prohibited wavelength the system flows into one of the closest allowed modulations. The overall structure is demonstrated in Fig. 3: close to an isolated point there is a basin of attraction, but further away from the bifurcation line these regions begin to overlap, and the sys-
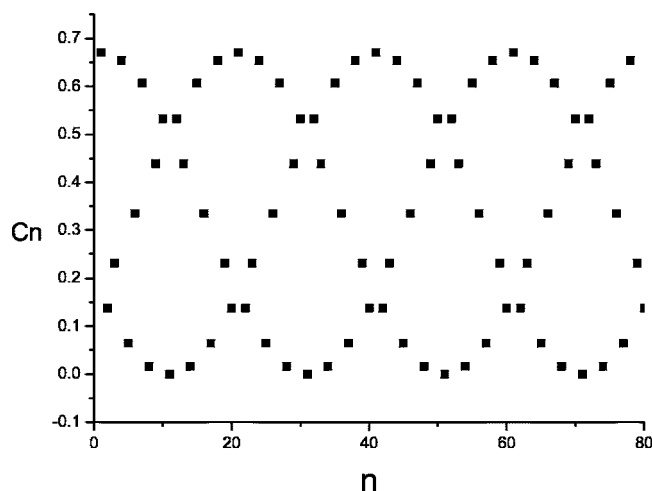
FIG. 2. Spatial structure of wave vector $k = 14\pi/20l_0$, where n is the site index and C_n is the concentration at each site. According to Eq. (14) one expects the modulation length to be $\lambda = 20l_0/7$, but discreteness of the lattice allows only for commensurate periodicity of 20 sites.

tem flows into some mixture of the closest allowed states, depending on its initial conditions. Deep in region III many wave numbers are involved; the interaction parameters are relatively large, and instead of simple harmonic modulation the system flows, generically, into a spiky steady where the "living colonies" are separated by the interaction length and are not effected by the competition between patches.
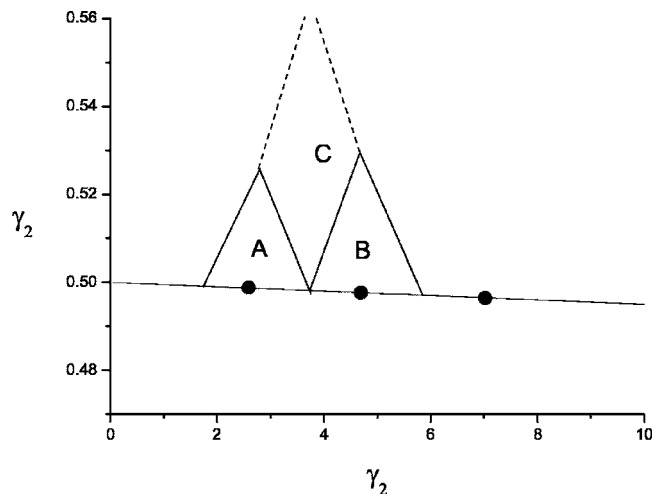

FIG. 3. Basins of attraction for allowed states close to the bifurcation line (sketched). The straight line is an enlarged portion of the bifurcation line (I-III interface) of Fig. 1. The bold points on this line correspond to an allowed state, i.e., states with wavelengths commensurate with the lattice size. Each possible wave vector admits a basin of attraction, like those denoted by A and B in the figure. Starting from γ_1, γ_2 values inside region A, for example, the system flows to the modulation correspond to the bold point inside the triangle. Away from the bifurcation line (region C) few basins of attraction overlap and mode competition takes place. Even further away, deep in region III, the system is in the spiky phase: many active modes exist and their superposition yields the "wave packet" characteristics of the spikes.

Although the numerical examples presented here are for a system with next nearest neighbor competition and without diffusion, it is easy to extract from it the properties of the steady state in general. The effect of diffusion is to increase the size of the stable region so the bifurcation line of Fig. 1 moves outward together with the pure and the spiky states as illustrated by the dashed line. For interactions of longer range the parameter space is of higher dimensionality; still, close to the origin (i.e., for weak competition) the homogeneous solution is stable, while far away (strong competition) one expects spatial segregation and the appearance of spikes, as discussed below.

III. DEFECTS

The transition from the homogeneous to the modulated state involves spontaneous breakdown of translational symmetry, and upon global initiation one may expect domain walls, or kinks, that separate spatial regions with different order parameter. The presence of these defects and their character is crucial for the understanding of the system response functions, e.g., its behavior under small noise: as there is no preference to one phase of the order parameter the kinks may move freely, while the "bulk" of the domain is much more stiff. In the following paragraphs the characteristic defects for various phases are presented.

A. Domain walls

As mentioned above, the nearest neighbor competition leads, above the bifurcation threshold, to appearance of an up-down modulation ($k = \pi$), and if there is no diffusion the steady state is the 0101010 configuration. Clearly there are two equivalent segregations of this type, namely, filled odd sites and empty even sites or vice versa. Accordingly, in the case of global initiation (random "seeds" are spread all around) one finds domains of the stable patterns with different parity, and domain walls (technically known as kinks or solitons) that separate these regions, as seen in Fig. 4. The nearest neighbor interaction is simple enough to allow for an analytic solution for the kink, and the numerical results confirm the predictions [6].

In the presence of diffusion there is a "smearing" of the above results: the homogeneous state is stable for larger γ, and above the segregation threshold the steady state is smeared from $\cdots 01010 \cdots$ to an "up-down-up-down" form, and the kinks are not of finite size but admit exponentially decaying tails; see Ref. [6] for details.

B. Phase shift

Unlike the nearest neighbor case, competition of longer range leads to instabilities with wavelengths of more than one site, i.e., $c_n = A_0 + A_k \cos(nkl_0)$ with general k. This opens the problem of defects between ordered regions. Inspired by the nearest neighbors example one may expect another types of kinks that separate different regions of ordered state. Surprisingly, this is not the case. Instead of getting kinks between different oriented regions of the activated wave number, one gets a *single* oriented region with *phase shift*,
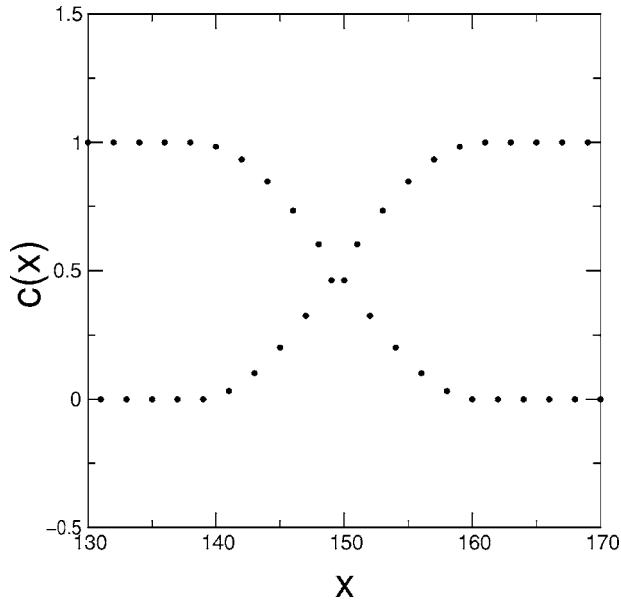
FIG. 4. A typical kink of length $L=20$, an outcome of forward Euler integration of Eq. (5) (with NN competition) on 1024 lattice points with periodic boundary conditions and random initial conditions at $\gamma=0.505$ (just above the bifurcation).

namely, the spatial structure is of the form $c_n=A_0+B\cos(nkl_0+\phi)$, where ϕ is the phase shift between the actual solution and the predicted modulation $c_n=A_0+A_k\cos(nkl_0)$ and $B=A_k/\cos\phi$.

On the unit cycle (Fig. 5) the meaning of this additional phase is a shift of all points by ϕ. This shift may reduce the number of distinct values in one cycle by 1, as indicated in
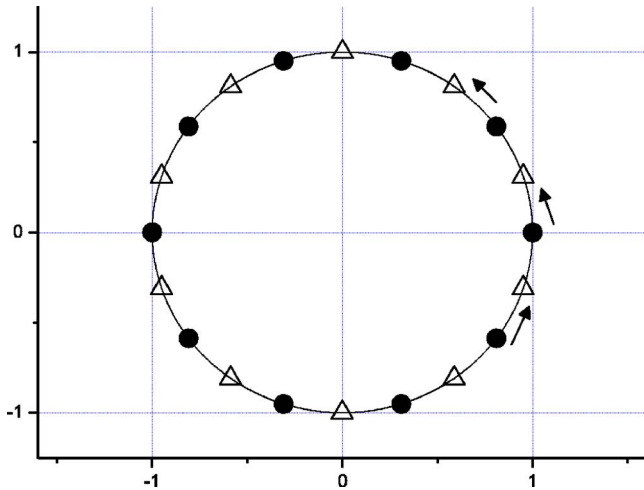

FIG. 5. (Color online) The set of different values of population size at different sites is presented on the unit circle where the linear analysis predicts an instability with wave number $k=3\pi/5l_0$. The filled circles are the values of $\cos(3n\pi/5l_0)$, the solution predicted by the naive argument, and this is indeed a stable solution with a finite basin of attraction (see Fig. 7). It turns out, however, that generic initial conditions flow into a phase shifted solution where the population is of the form $\cos(3n\pi/5l_0+\phi)$ (shown in Fig. 8). The value of ϕ is half of the angular distance between two close sites, here corresponds to the open triangles on the unit cycle.

the example of Fig. 5: here, instead of six distinct values taken by c_n along one wavelength, there are only five. Both numerical simulations of the system dynamics, starting from random initial conditions, and stability analysis of the possible steady state for arbitrary ϕ indicates that, although any ϕ corresponds to a locally stable solution, the most stable ϕ equals half of the angular distance between two adjusting points on the circle. In Fig. 5 the actual phase shifted pattern is shown for $k=3\pi/5l_0$, while Fig. 6 indicates that the most stable phase corresponds to $\phi/\phi_0=1$. As the Lyapunov exponent of any ϕ is negative, small perturbations around any ϕ value (in particular, $\phi=0$) decay. Figure 7 shows the corresponding stable mode with $\phi=0$ where the initial conditions are small perturbations around it. Figure 8, on the other hand, shows the final state with generic initial conditions, where the system flows to the most stable pattern with $\phi/\phi_0=1$.

IV. SPIKY PHASE

Deep in region III of the phase diagram (Fig. 1) many wave vectors are excited, with strong mode competition between them, and the linear analysis picture based on Fourier decomposition becomes ineffective. Better insight into the system comes from a real space analysis: deep into region III the long-range competition is strong, and within the effective interaction range a new colony cannot develop in the presence of a fully grown one. Accordingly, this phase is characterized by fully developed colonies separated by "dead regions" of constant length that reflect the effective interaction length. In Fourier space, this corresponds to many active modes that build together a periodic structure of "bumps."

In the case of global initiation, of course, defects may appear in the stable steady state as the system flows to different order parameters in different regions. Again, it is better to use the real space picture in order to describe these defects. The situation is close to what is observed in the case of random sequential adsorption [21,27]: while an "optimal" filling of the system admits a periodic structure of living patches with periodicity of, say, L lattice points, it may happen that the distance between two fully developed sites is between L and $2L$, and all the site in between should remain empty due to the long-range competition. The emerging spatial configuration is of ordered regions (with coherence size that depends upon the dynamics) separated by "domain walls," where the width of these walls is taken from some distribution function between zero and the interaction effective length.

V. TWO DIMENSIONAL SYSTEM

Although all the analysis presented was in one dimension, the basic picture is the same for higher dimensionality. In particular, the bifurcation condition is similar, nearest neighbor interactions yield a "checkerboard" phase above the bifurcation line, and the spiky phase is also observed.

For nearest neighbor interaction kinks between different regions (checkerboard parity) occurs. Because of the two dimensionality of the lattice the kinks might have any arbitrary
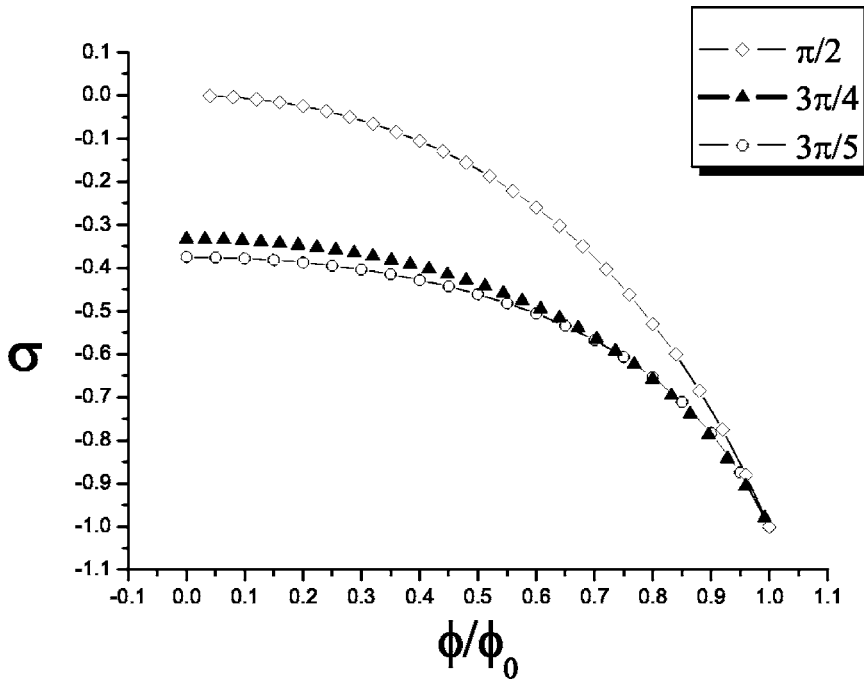
FIG. 6. The Lyapunov exponent (σ) (in arbitrary units) the phase shift for various wave numbers, i.e., for solutions of the form $\cos(nk+\phi)$. While the steady state is stable for any ϕ, the most stable state corresponds to ϕ_0, half of the angular distance between two consecutive lattice points.

spatial line, rather than straight line, as shown in Fig. 9. Those kinks are *de facto* one dimensional (1D) topological defects, because of the periodic boundary conditions. On the other hand, the domain walls of Fig. 10 seems to admit a real 2D features, although their topological character is not clear.

VI. GLOBAL PROPERTIES

A. Upper critical diffusion

Let us turn back to the bifurcation condition, Eq. (11), in different representation:

$$\frac{\beta_k}{\beta_0} + 2D[1 - \cos(kl_0)] < 0, \tag{17}$$

where the k considered is the one for which β_k admits a global minimum. Clearly, this k_{min} depends only on the form of the interaction kernel and is independent of its strength (if one multiplies all γ_r by a constant factor, the value of k_{min} remains the same). Since the negative term in the instability condition β_k/β_0 cannot exceed (-1), the absolute value of the right hand term should be even smaller to allow a periodic modulation of the stable steady state.
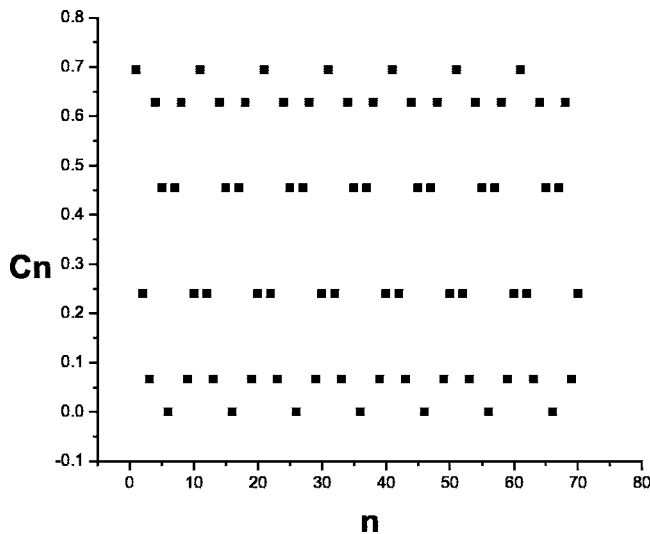

FIG. 7. The steady state (for the parameters of Fig. 5) where n is the site index and c_n is the concentration at each site. The initial conditions are close to the $\phi=0$ solution, i.e., $c_n(t=0)=A_0 + A_k \cos(3\pi n/5) + \delta_n$, where δ_n is a small random number. The system flows to the $\phi=0$ steady state, in agreement with the local stability analysis presented in Fig. 6.
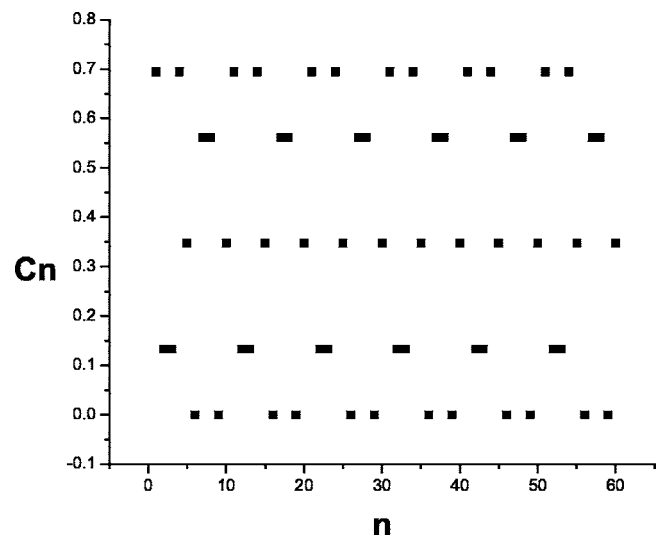

FIG. 8. Same as Fig. 7, but now the initial conditions are generic, $c_n(t=0)=\delta_n$. The system flows to the most stable steady state that corresponds, in this case, to $c_n=A_0+B\cos(3n\pi/5+\phi)$, with $\phi=3\pi/10$.
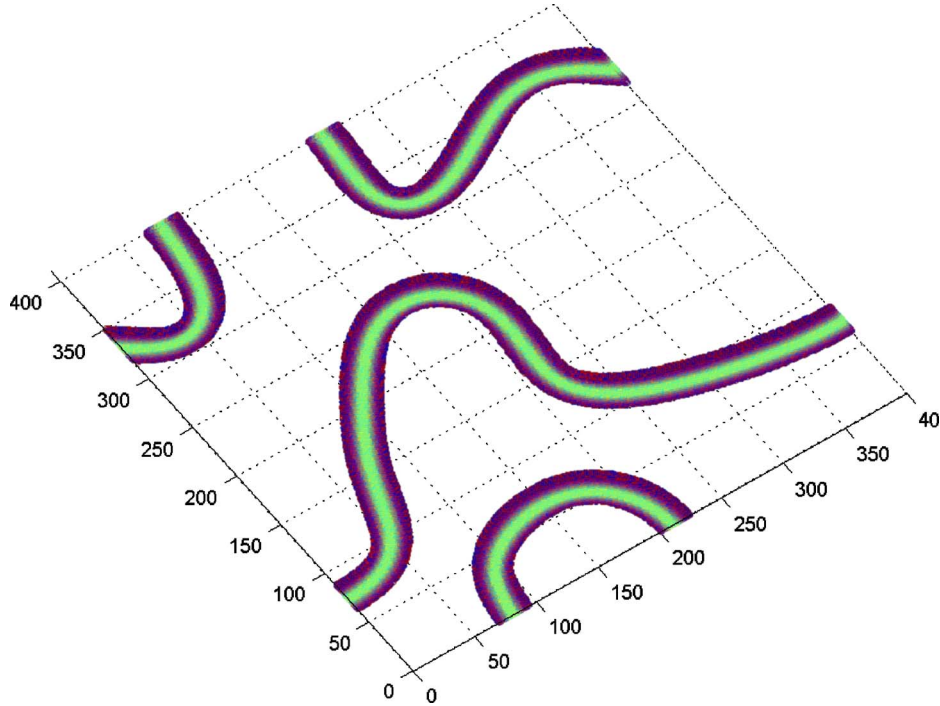
FIG. 9. (Color online) Spatial domains in a two dimensional system, for logistic growth with nearest neighbor competition. The parameters are chosen to be above the bifurcation threshold, and the stable steady state is a checkerboard with alternating filled and empty sites. Denoting a site by its coordinates i, j, there are two possible phases of the solution, corresponding to filled $i+j$ odd, empty $i+j$ even, and vice versa. Here, the results of a Euler integration of the process for a 2D sample of 50×50 sites with periodic boundary conditions is presented, where only the kinks separating regions of different order parameters are colored. The kinks here are noncontractible on the torus and correspond to one dimensional topological defects. The simulation parameters are $D=0$, $\gamma_1 = 0.2505$. Initial conditions are seed populations at each site taken randomly from a square distribution between $[0,0.01]$.

Assume, now, that the wavelength of the modulation is much larger than the lattice constant (as already required as one approaches the the continuum limit). In that case the approximation $2D[1 - \cos(kl_0)] \approx Dk_{min}^2 l_0^2$ holds, and since $D = (W_F/l_0)^2$, this term is proportional to $(W_F/\lambda)^2$, where λ is the period of the modulation. This implies that, independent of the strength of the long-range competition, *bifurcation never takes place if the width of the Fisher front is larger than the period of the modulation*. This statement holds up to a numerical factor (between 0 and 1) which is determined by the form of the competition kernel.

A simple example that demonstrates these considerations is the case of nearest neighbor interaction. Here

$$g(k) = 1 + 2\gamma \cos(k) + 2(1 + 2\gamma)D[1 - \cos(kl_0)] \quad (18)$$

and the global minima is $k = \pi$. $g(k_{min})$ is

$$g(\pi) = 1 - 2\gamma + 4(1 + 2\gamma)D \quad (19)$$

so for any γ there is an upper critical D,

$$D_c = \frac{2\gamma - 1}{4(1 + 2\gamma)}, \quad (20)$$

above which no bifurcation takes place. This upper critical diffusion constant converges to a global value as $\gamma \to \infty$,

$$D_c^g \equiv D_{c,\gamma->\infty} = \frac{1}{4}, \quad (21)$$

and no bifurcation takes place when the width of the Fisher front is of the order of the modulation length. Intuitively this result may be understood as follows: suppose that the system is in its 010101 state, and suppose that the dynamics is discrete in time. If $D=1/4$ it implies that each filled site contributes $1/4$ to any of its neighbors, and then the system is frozen in its homogeneous state with amplitude $1/2$ at each site. Generalizing this intuition to periodic modulation of arbitrary wavelength yields the same result, where the Fisher front width stands as a definition of an "effective site."

B. Spatial segregation and total population

Given a system with long range competition, one may ask how the *total* population (integrated over all the spatial domain) or the average population density depend on the phase of the system. As pointed out by Refs. [7,15], for a system of discrete agents with nonlocal interactions, the size of the total population depends on the efficiency of segregation: strong segregation implies higher population (on average, since there are empty regions and living patches). Thus the decrease of diffusion implies a higher total population density. In this subsection this phenomenon is analyzed at the rate equation limit on a lattice with different interaction range and dimensionality.
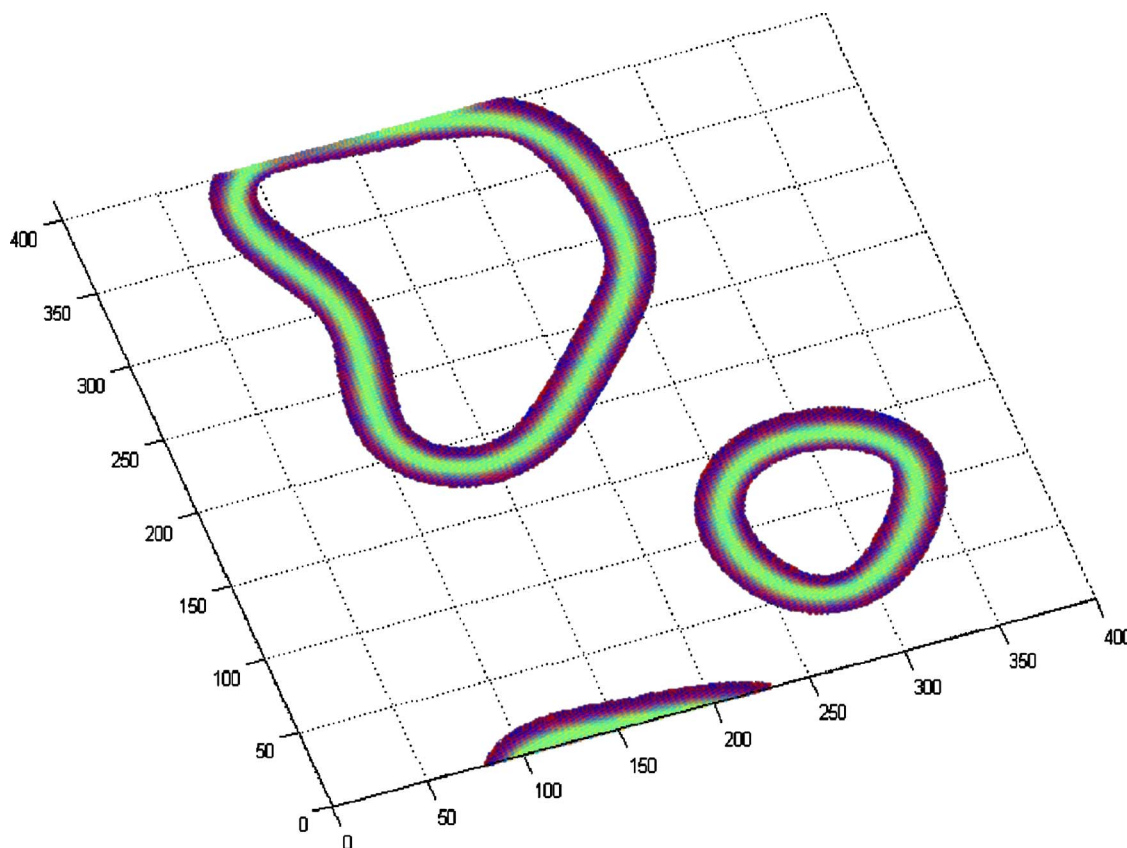
FIG. 10. (Color online) The same system and parameters as in Fig. 9, for another choice of random initial conditions. Here the domain wall is contractible on the torus and the order parameter phases are different between the inside and the outside of the kink.

Clearly, the total population is given by the amplitude of the zero mode in Fourier decomposition of the population [see Eq. (6)]. As long as the system is in its homogeneous phase this quantity is diffusion independent and the total population depends only on the strength of the interaction, $A_0 = 1/\beta_0$. Right above the bifurcation, when only one excited mode (k) exists, the total population is proportional to $A_0 = \alpha_k/(\beta_0 + \beta_k)$, and since α_k increases as D decreases, so does the total population. In the case of one dimensional lattice with nearest neighbor interaction, for example, the dependence of the total occupancy of the sample on the diffusion constant may be calculated explicitly, since there is only one excited mode $k = \pi/l_0$. Here even far from the bifurcation point the amplitude of the zero mode is given by $A_0 = \alpha_k/(\beta_0 + \beta_k)$. The total sum vs diffusion is, accordingly,

$$A_0 = \begin{cases} (1 - 4D)/2, & D < D_c \\ 1/(1 + 2\gamma), & D > D_c. \end{cases} \quad (22)$$

Figure 11 shows the total sum vs diffusion for few situations. The numerical results indicate that the decay of average population is approximately linear. Note that, for the "top hat" competition presented here, there seems to be a discontinuity at D_c in two dimensions, while in one dimension the total population is continuous at the transition.

VII. LOCAL INITIATION: DYNAMICS OF INVASION AND SEGREGATION

In this paper, an analysis of the stable steady states of the logistic growth with long range competition was presented. As few stable steady solutions may exist simultaneously for the same set of parameters, the generic situation was identified numerically using global initiation, i.e., a small random population at each site. In this section, the dynamics of growth is analyzed, where the initial conditions are a colony with compact support. For local logistic growth this problem was considered years ago by Fisher [16] and Kolomogorov [17]. The invasion of the stable solution into the unstable one takes place via a front (the Fisher front) that propagates in constant velocity. This problem was considered by many authors in different contexts and was generalized to other cases of invasion into an unstable state; see the comprehensive review by van Saarloos [19].

The effects of nonlocal competition on the propagation and shape of the Fisher front was considered by Gourley [29] for the case of the stable homogeneous solution. While the nonlocal competition has no effect on the front velocity [since the velocity of a pulled wave depends only on the linear parts of Eq. (2)], it has an effect on the shape of this front. Close to the front edge the effective competition is smaller (as there is no competition from the almost empty sites at the leading edge). As a result, the leading edge is
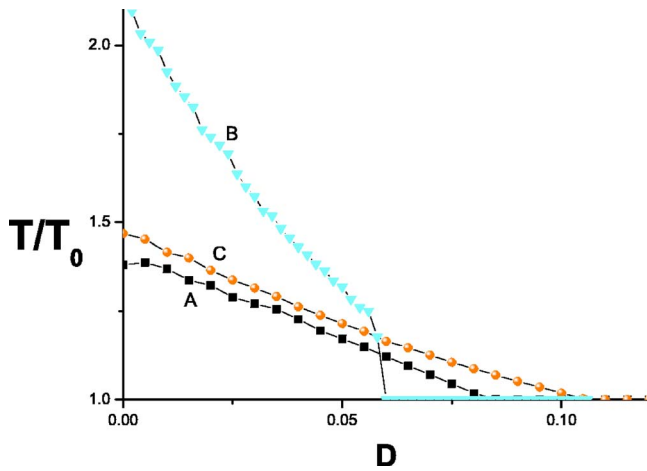
FIG. 11. (Color online) Total population (**T**) vs diffusion coefficient (**D**) for several situations. (A) 1D with nearest neighbor interaction (squares). (C) 1D, NNN interaction (circles). (B) 2D, top hat interaction (triangles). The top hat is constant interaction with all sites inside a circle of radius $3l_0$, and zero outside. In order to present all the results in the same panel, the population has been normalized, for each system, by its homogeneous solution (T_0).

followed by a "hump" of higher biomass, as can be seen here, especially in Fig. 12.

As emphasized above, the system considered here may admit (in regions II and III of Fig. 1) two instabilities: the empty state is unstable against the homogeneous one, while the homogeneous solution breaks and yields a spatial modulation. Accordingly, if the system is initiated locally from a small colony of compact support one expects that two fronts propagate into the empty region: first the front associated with the homogeneous state, and then the modulation (secondary instability) front [30]. These two fronts travel in different velocities. Generally, it is known that the Fisher veloc-
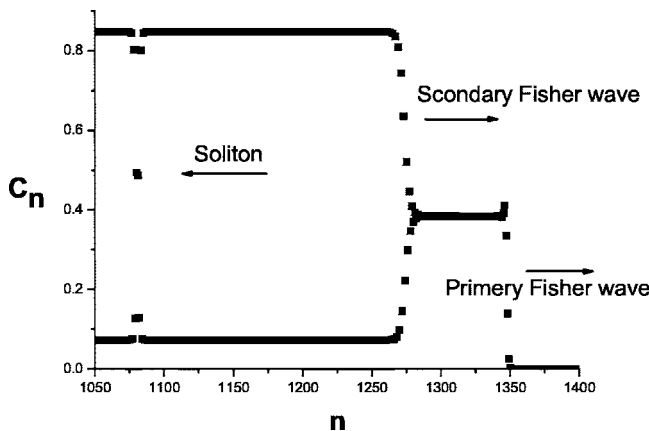

FIG. 12. Snapshot of the one dimensional system, initiated locally from the left, where the primary velocity is higher than the secondary velocity. The two fronts are clearly shown, and the homogeneous region between them is widening as time elapsed. The simulation assumes nearest neighbor competition with $D=0.04$ and $\gamma=0.8$. Along time, defects (one shown left to the front) are generated at the tip of the secondary front due to the noise induced by the primary front.
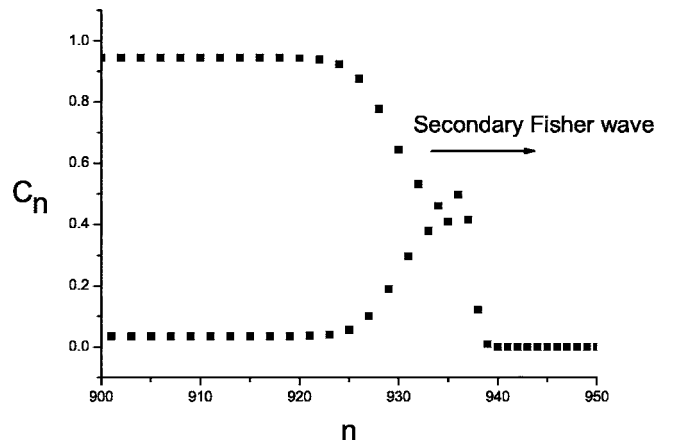

FIG. 13. The same as Fig. 12, but now the velocity of the secondary front is higher than the velocity of the primary front. Since the secondary instability may appear only after the primary, the velocity of the whole front is determined by v_p. The parameters used are $D=0.005$, $\gamma=0.65$.

ity is determined by the leading edge ("pulled" fronts) and is related to the Lyapunov exponent that characterizes the relevant instability. Accordingly, the dynamics of our system is determined by two velocities: v_p, the velocity of the primary front (that interpolates between the empty and the homogeneous state) and the modulation velocity v_s. While v_p is γ independent, the secondary front velocity v_s depends on the characteristics of the long range competition. By tuning of γ, though, one may change the relative velocity between the primary and the secondary front. Both velocities may be calculated analytically using a saddle point method and taking into account the discreteness of the lattice points, as discussed in the Appendix. Generically, there are two possible scenarios for the takeover of an empty region by spatially modulated steady state: in the first case $v_p > v_s$ (see Fig. 12) and the homogeneous region between the primary and the secondary front grows linearly in time. This situation is very sensitive, as small perturbations (induced by the leading front) lead to spontaneous bifurcation of the homogeneous region, a process that yields many structural defects (e.g., kinks) along the chain.

In the second case the situation is different: if $v_p < v_s$ there is no homogeneous region, and only one front exists. Its velocity is determined, of course, by the primary front velocity, but its shape is different (see Fig. 13). In that case the sensitive homogeneous region never exists, and the pattern formation process is robust, with no defects associated with the front kinetics.

VIII. CONCLUSIONS AND REMARKS

This paper attempts to present the various phases associated with the steady states of the logistic process on spatial domains with nonlocal competition. The main feature is, of course, the segregation transition that happens, as was shown, where the width of the Fisher front (associated with the homogeneous solution) becomes shorter than the instability wavelength. Right above the bifurcation one finds a

pattern dominated by a single wavelength, while far away from the bifurcation line the stable steady state becomes spiky. Each phase is associated with its own defects: phase shift close to the bifurcation, empty regions in the spiky phase, and domain walls (kinks) for the up-down phase of the nearest neighbor interaction. It turns out that the segregation transition increases the overall carrying capacity per unit volume. In one dimension the population continues at the transition while in two dimensions discontinuity might occur.

Upon local initiation the system dynamics is governed by the relations between the velocities of the primary (empty to homogeneous) and the secondary (homogeneous to modulated) fronts. The numerics suggests that, while global initiation may yield "disordered" structure with many defects per unit length, local initiation with the same parameters yields ordered structure unless the secondary front velocity is smaller that the primary one.

While in this work only rate equations of reaction-diffusion type have been considered, in recent numerical works of Birch and Young [15] and Garcia *et al.* [7] the stochastic motion of the individual reactants is taken into account. These stochastic models add two ingredients to the description presented here. First, the introduction of individual reactants ("Brownian bugs" [31]) implies a *threshold* on the reactant concentration on a single patch. Second, there is a multiplicative noise associated with the stochastic motion of individual reactants. As shown in this work, many of the features associated with long-range competition are independent of the discrete nature of individual reactants[28].

ACKNOWLEDGMENTS

APPENDIX

In this Appendix the analytic expression for the secondary front velocity on a discrete lattice is obtained, via the saddle point argument (see Ref. [32]). For the sake of simplicity, only the case of nearest neighbor interaction is considered. In order to perform the same calculations for competition beyond the NN limit, one should first find numerically the steady state modulation and then follow the same procedure.

The evolution of a population is given by

$$\frac{\partial c_n}{\partial t} = D[-2c_n + c_{n+1} + c_{n-1}] + c_n - c_n^2 + c_n\gamma(c_{n+1} + c_{n-1}).$$

(A1)

Denoting by δ_n the deviations from the homogeneous solution, $c_n = A_0 + \delta_n$, Eq. (A1) is linearized to yield

$$\frac{\partial \delta_n}{\partial t} = \alpha\delta_n + \beta(\delta_{n+1} + \delta_{n-1}),$$

(A2)

where $\alpha = a - 2bA_0 + 2A_0\gamma - 2D$ and $\beta = D - A_0\gamma$. Assuming a modulated solution of the form
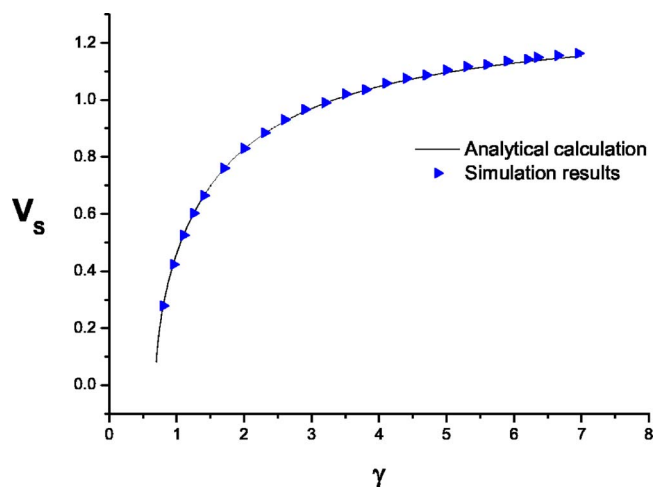

FIG. 14. (Color online) Comparison of the numerical simulation (triangles) and the theoretical prediction based on the saddle point method [Eqs. (A8) and (A9), solid line] for the velocity of the secondary front as a function of the interaction strength. The diffusion used is $D = 0.04$ and the lattice constant is $l_0 = 1$, $dt = 0.01$.

$$\delta_n = \begin{cases} Ae^{ikl_0 n + \Gamma(k)t}, & n \text{ odd} \\ Be^{ikl_0 n + \Gamma(k)t}, & n \text{ even} \end{cases}$$

(A3)

and plugging Eq. (A3) into Eq. (A2) one gets

$$\Gamma(k)\begin{bmatrix} A \\ B \end{bmatrix} = \begin{bmatrix} \alpha & \beta\cos(kl_o) \\ \beta\cos(kl_o) & \alpha \end{bmatrix}\begin{bmatrix} A \\ B \end{bmatrix}.$$

(A4)

The dispersion relations are given by

$$\Gamma(k) = \alpha + \beta\cos(kl_0),$$

(A5)

where the plus sign is chosen for the unstable modes. The solutions are of the form

$$\begin{bmatrix} c_n \\ c_{n+1} \end{bmatrix} = \begin{bmatrix} A \\ B \end{bmatrix}e^{ikx + \Gamma(k)t}.$$

(A6)

If a solution represents a traveling front with velocity v it is useful to define the coordinate system in the moving frame, $\zeta = x - vt$, to get

$$\begin{bmatrix} c_n \\ c_{n+1} \end{bmatrix} = \begin{bmatrix} A \\ B \end{bmatrix}e^{ik\zeta + ikvt + \Gamma(k)t}.$$

(A7)

Using the saddle point method [19] the two equations that determine the velocity are

$$f \equiv ivk + \alpha + 2\beta\cosh(kl_0) = 0$$

(A8)

and

$$\frac{\partial f}{\partial k} = iv + 2\beta_0\sinh(kl_0) = 0.$$

(A9)

In the case of finite time steps one should replace ivk by $(e^{-ikvdt} - 1)/\delta t$ to get the appropriate corrections. Figure 14 shows the perfect fit between the solution of Eqs. (A8) and (A9) and the numerical solution.

[1] N. F. Britton, J. Theor. Biol. **136**, 57 (1989).
[2] N. F. Britton, SIAM J. Appl. Math. **50**, 1663 (1990).
[3] S. A. Gourley and N. F. Britton, J. Math. Biol. **34**, 297 (1996).
[4] H. Sayama, M. A. M. de Aguiar, Y. Bar-Yam, and M. Baranger, Phys. Rev. E **65**, 051919 (2002).
[5] M. A. Fuentes, M. N. Kuperman, and V. M. Kenkre, Phys. Rev. Lett. **91**, 158104 (2003).
[6] N. M. Shnerb, Phys. Rev. E **69**, 061917 (2004).
[7] E. Hernandez-Garcia and C. Lopez, Phys. Rev. E **70**, 016216 (2004).
[8] D. Iron and M. J. Ward, SIAM J. Appl. Math. **60**, 778 (2000).
[9] A. Sakai, J. Theor. Biol. **186**, 415 (1997).
[10] M. Doebeli and T. Killingback, Theor Popul. Biol. **64**, 397 (2003).
[11] B. M. Bolker, Theor Popul. Biol. **64**, 255 (2003).
[12] K. Tokita and A. Yasutomi, Theor Popul. Biol. **63**, 131 (2003).
[13] K. Anderson and C. Neuhauser, Ecol. Modell. **155**, 19 (2002).
[14] F. Hoops *et al.*, J. Theor. Biol. **210**, 201 (2001).
[15] D. Birch and W. R. Young (private communication).
[16] R. A. Fisher, Ann. Eugenics **7**, 353 (1937).
[17] A. Kolomogoroff, I. Petrovsky, and N. Piscounoff, Moscow Univ. Bull. Math. **1**, 1 (1937).
[18] E. Brunet and B. Derrida, J. Stat. Phys. **103**, 269 (2001).
[19] See, e.g., W. van Saarloos, Phys. Rep. **386**, 29 (2003).
[20] J. B. Wilson and A. D. Q. Agnew, Adv. Ecol. Res. **23**, 263 (1992); R. Lefever and O. Lejeune, Bull. Math. Biol. **59**, 263 (1997); J. von Hardenberg, E. Meron, M. Shachak, and Y. Zarmi, Phys. Rev. Lett. **87**, 198101 (2001).
[21] N. M. Shnerb, P. Sarah, H. Lavee, and S. Solomon, Phys. Rev. Lett. **90**, 038101 (2003).
[22] A. Manor and N. M. Shnerb (unpublished).
[23] F. J. Weissing and J. Huisman, J. Theor. Biol. **168**, 323 (1994).
[24] K. S. McCann, J. B. Rasmussen, and J. Umbanhower, Ecol. Lett. **8**, 513 (2005).
[25] P. Bak and R. Bruinsma, Phys. Rev. Lett. **49**, 249 (1982).
[26] D. R. Nelson and N. M. Shnerb, Phys. Rev. E **58**, 1383 (1998), Appendix B.
[27] See, e.g., J. Talbot, G. Tarjus, P. R. Van-Tassel, and P. Viot, Colloids Surf., A **165**, 287 (2000), and references therein.
[28] E. H. Garcia and C. Lopez, Physica D **199**, 223 (2004).
[29] S. A. Gourley, J. Math. Biol. **41**, 272 (2000).
[30] See, e.g., M. C. Cross and P. Hohenberg, Rev. Mod. Phys. **65**, 851 (1993), and references therein.
[31] W. R. Young, A. J. Roberts, and G. Stuhne, Nature (London) **412**, 328 (2001).
[32] L. Pechenik and H. Levine, Phys. Rev. E **59**, 3893 (1999).